Archival Report

Biological Psychiatry

Cytoplasmic FMR1-Interacting Protein 2 Is a Major Genetic Factor Underlying Binge Eating

Stacey L. Kirkpatrick, Lisa R. Goldberg, Neema Yazdani, R. Keith Babbs, Jiayi Wu, Eric R. Reed, David F. Jenkins, Amanda F. Bolgioni, Kelsey I. Landaverde, Kimberly P. Luttik, Karen S. Mitchell, Vivek Kumar, W. Evan Johnson, Megan K. Mulligan, Pietro Cottone, and Camron D. Bryant

ABSTRACT

BACKGROUND: Eating disorders are lethal and heritable; however, the underlying genetic factors are unknown. Binge eating is a highly heritable trait associated with eating disorders that is comorbid with mood and substance use disorders. Therefore, understanding its genetic basis will inform therapeutic development that could improve several comorbid neuropsychiatric conditions.

METHODS: We assessed binge eating in closely related C57BL/6 mouse substrains and in an F_2 cross to identify quantitative trait loci associated with binge eating. We used gene targeting to validate candidate genetic factors. Finally, we used transcriptome analysis of the striatum via messenger RNA sequencing to identify the premorbid transcriptome and the binge-induced transcriptome to inform molecular mechanisms mediating binge eating susceptibility and establishment.

RESULTS: C57BL/6NJ but not C57BL/6J mice showed rapid and robust escalation in palatable food consumption. We mapped a single genome-wide significant quantitative trait locus on chromosome 11 (logarithm of the odds = 7.4) to a missense mutation in cytoplasmic FMR1-interacting protein 2 (*Cyfip2*). We validated *Cyfip2* as a major genetic factor underlying binge eating in heterozygous knockout mice on a C57BL/6N background that showed reduced binge eating toward a wild-type C57BL/6J-like level. Transcriptome analysis of premorbid genetic risk identified the enrichment terms morphine addiction and retrograde endocannabinoid signaling, whereas binge eating resulted in the downregulation of a gene set enriched for decreased myelination, oligodendrocyte differentiation, and expression.

CONCLUSIONS: We identified *Cyfip2* as a major significant genetic factor underlying binge eating and provide a behavioral paradigm for future genome-wide association studies in populations with increased genetic complexity.

Keywords: Anxiety, Binge, Eating disorders, GWAS, Myelin, Prader-Willi syndrome

http://dx.doi.org/10.1016/j.biopsych.2016.10.021

Eating disorders (ED) are among the most lethal psychiatric disorders and exhibit a lifetime prevalence of 1–3% (1). Binge eating disorder (BED) is frequently associated with severe obesity, metabolic dysfunction, and increased mortality (1,2). Both genetic and environmental factors contribute to binge eating (BE) (3); however, genome-wide association studies in humans are currently limited in their power to detect the contribution of common variants (4). BE, defined by the uncontrolled overconsumption of a large amount of food within a brief time period (usually energy-dense palatable food [PF]), is one of the most highly heritable traits associated with ED, including BED (5), bulimia nervosa (6), and a subset of cases of anorexia nervosa (7). Focusing on the genetic and biological basis of a single trait such as BE that is presumed to comprise less genetic and biological complexity than an aggregate disorder could be a more tractable goal toward gene identification (5,8) and accelerate the development of new therapeutics.

ED are comorbid with anxiety traits (9), mood disorders, obsessions/compulsions, impulse control, and substance use disorders, suggesting shared genetic factors (1). Recent theories of BE have adopted theories of addiction to explain its compulsive basis and the underlying genetic and neural mechanisms (10–12). Compulsive BE shares several features with addiction, including an escalation in consumption, physiological and emotional-affective dependence, cue-induced craving, and relapse (12).

Neurochemical mechanisms of BE converge on activation of the mesocorticolimbic dopamine system (13,14). Cue-induced craving correlates with BE in humans (15) and changes in extracellular dopamine in the dorsal striatum in response to food stimuli correlate with scores of BE severity in patients with BED (16). The dorsal striatum processes food sensation and reward (17), for example the nutritional value of sugar (18) and enkephalin-mediated coding of sensory reward induced by PF consumption (19,20). Furthermore, the volume

SEE COMMENTARY ON PAGE e77

ISSN: 0006-3223

of the dorsal striatum is reduced in patients with anorexia and bulimia and correlates with predicted sensitivity to reward (21). Finally, recruitment of the dorsal striatum combined with a loss of prefrontal cortical inhibition is hypothesized to mediate a shift to habitual, cue-responsive compulsive-like behaviors associated with addiction (22), including BE (10).

Quantitative trait locus (QTL) mapping is a genome-wide, discovery-based approach to uncover novel genetic and biological mechanisms of complex traits such as BE (23–25). In mice, millions of genetic variants typically distinguish commonly used inbred strains (26), highlighting one of the challenges to identifying causal genetic variants. To help overcome this particular challenge, closely related substrains exhibiting extreme phenotypic and little genetic diversity can be employed to facilitate gene mapping (27,28). C57BL/6 (B6) substrains show robust differences in behavioral responses to drugs of abuse (28) and whole-genome sequencing identified only approximately 10,000 single nucleotide polymorphisms that distinguish C57BL/6NJ (B6NJ) and C57BL/6J (B6J) strains (26). This drastically reduced genetic complexity can facilitate identification of causal genetic factors (29). Behavioral differences between B6J and B6NJ combined with whole-genome sequence information make these strains an attractive and accessible model for identifying the genetic basis of variation in complex traits. However, whether these strains differ in BE has not been examined.

Here, we developed an intermittent, limited access procedure for BE in a conditioned place preference (CPP) paradigm using outbred Swiss Webster (CFW) (Charles River Laboratories, Wilmington, MA) mice. We identified a robust difference in BE between B6 substrains and used QTL mapping and gene targeting to identify a major genetic factor associated with BE. Finally, we used striatal transcriptome analysis via messenger RNA sequencing in a subset of F_2 mice and heterozygous gene knockout mice to gain insight into the premorbid neurobiological mechanisms that bridge genetic variation with BE susceptibility and the neurobiological adaptations induced by BE.

METHODS AND MATERIALS

Mice

All experiments were performed in accordance with the National Institutes of Health Guidelines for the Use of Laboratory Animals and were approved by the Institutional Animal Care and Use Committee at Boston University. CFW mice (7 weeks old) were purchased from Charles River Laboratories (Crl: CFW [SW]) and were used to choose the PF diet (20-mg pellets; 5-TUL, TestDiet, St. Louis, MO) and design the BE and PF-CPP paradigm (Supplement). C57BL/6J (B6J) and C57BL/NJ (B6NJ) mice (7 weeks old) were purchased from the Jackson Laboratory (Bar Harbor, ME). Details on purchased mice and on B6J × B6NJ-F_1, -F_2, and heterozygous *Cyfip2* knockout mice (*Cyfip2*$^{N/-}$) are provided in the Supplement.

BE and PF-CPP

We chose a BE CPP design to examine both the consummatory and the conditioned motivated behaviors associated with BE. The long-term goal is to identify shared and divergent genetic factors that mediate these behaviors using forward genetics. We used a two-chamber CPP design (30) to measure BE and PF-CPP on day (D) 1–D22 (see Figure 1). On D23, F_2 mice received a final PF training session and on D24 mice were tested on the elevated plus maze for 5 minutes (Supplement) and sacrificed for collection of striatum punches (31). For the knockout study, *Cyfip2*$^{N/-}$ and *Cyfip2*$^{N/N}$ mice were tested for compulsive-like eating in the light/dark conflict test on D23 (see below) and sacrificed on D24 (24 hours later) for collection of striatum punches (31). Mice homozygous for the *Cyfip2* knockout allele are lethal at postnatal day 1.

Light/Dark Conflict Test

The light/dark conflict test was employed on D23 as a measure of compulsive-like eating (32) in *Cyfip2*$^{N/N}$ and *Cyfip2*$^{N/-}$ mice. One side is black opaque Plexiglas whereas the other side is transparent and light exposed with a small doorway allowing access to both sides. The light side is an aversive, bright compartment that the mice normally avoid. We operationalized an increase in PF consumption on the light side despite adverse conditions as a construct of compulsive-like eating (32). A porcelain bowl containing PF (5-TUL pellets) was placed into the center of the light side and each mouse was placed on the light side facing the food bowl and the doorway. Time on the light side, amount of PF consumed, and entries were recorded for 30 minutes.

Behavioral Analysis of BE in CFW, B6J, and B6NJ Mice

Behavioral analysis was conducted in R (https://www.r-project.org/) using mixed-model analyses of variance (genotype, treatment, and sex as independent variables; day as a repeated measure) with an alpha level of .05 to detect main effects and interactions. Primary outcome measures included percent body weight consumed and time spent on the PF-paired side. We also determined differences in the slope (rate) of escalation in PF consumption as an additional measure of BE (33). Post hoc analyses following main effects and interactions were performed using one- or two-way analyses of variance, and Welch's unequal variances t tests ($p < .05$, Bonferroni corrected for the number of comparisons made).

QTL Analysis of B6J × B6NJ-F_2 Mice

F_2 mice were genotyped using a custom Fluidigm genotyping array (South San Francisco, CA) with 96 single nucleotide polymorphisms (26,29). QTL analysis was conducted in R/qtl (scanone) using Haley-Knott regression and 1000 permutations to establish significance thresholds ($p < .05$, error probability = .0001) (34). We also analyzed female ($n = 78$) and male mice ($n = 78$) separately. The marker position (cM) was estimated using the sex-averaged position from the Mouse Map Converter (http://cgd.jax.org/mousemapconverter) (35).

Behavioral Analysis of *Cyfip2*$^{N/-}$ Mice

We used a 2 × 2 factorial design to measure PF versus chow consumption as a function of genotype (*Cyfip2*$^{N/N}$, *Cyfip2*$^{N/-}$; 59–61 days old on D1). Chow consisted of 20-mg pellets (TestDiet, St. Louis, MO) that contained a nearly identical nutritional profile to the PF with the exception that they lacked sucrose. A minimum sample size of $n = 20$ was employed based on 80% power ($p < .05$; Supplement). Mice were

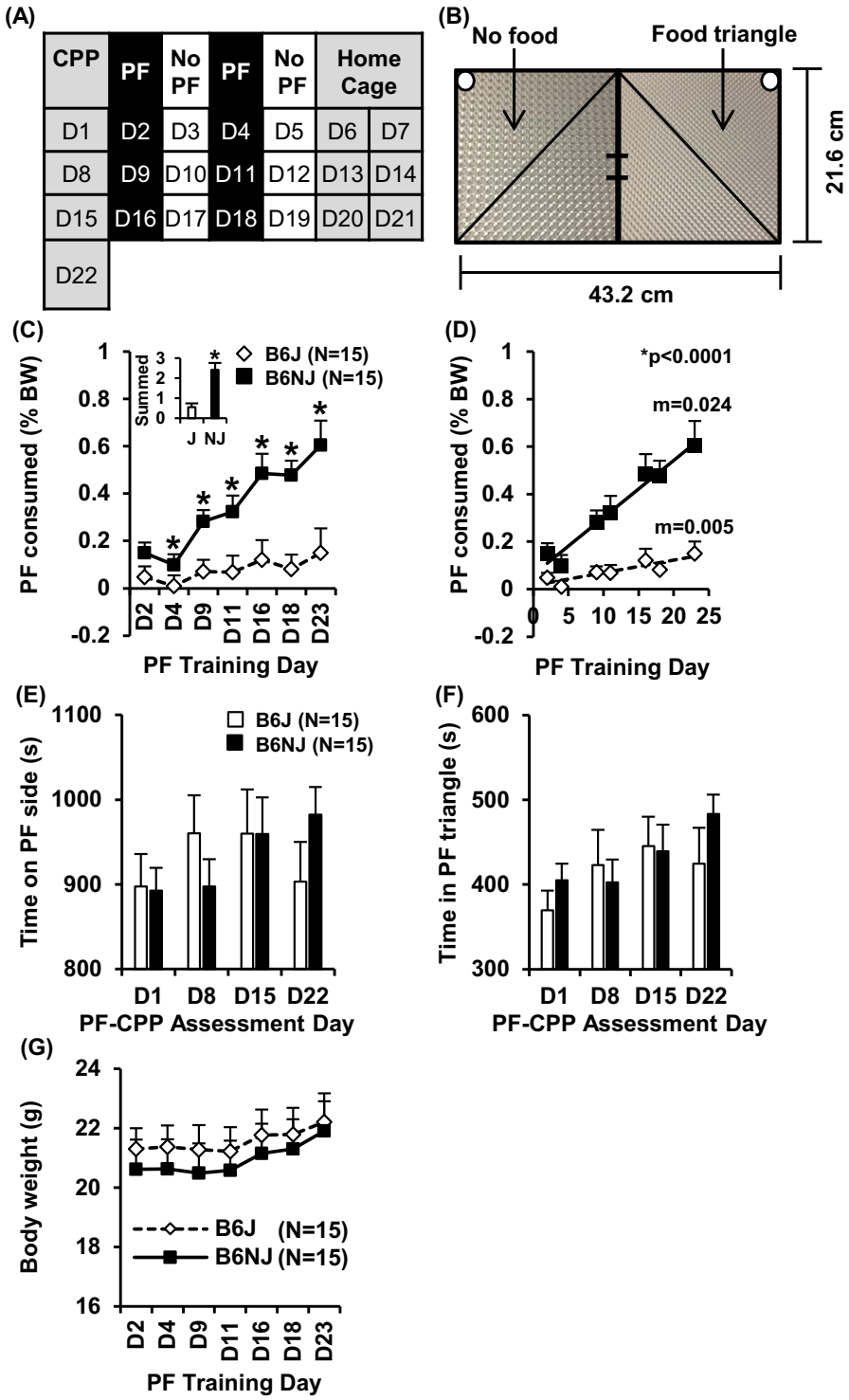

Figure 1. Escalation of palatable food (PF) consumption in C57BL/6NJ (B6NJ) but not C57BL/6J (B6J) mice. Mice were video recorded and video tracked in unlit sound-attenuating chambers for preference for the PF-paired side (right side). On day (D) 1, mice were assessed for initial preference whereby mice were placed into the left side and provided free access to both sides (30) that contained clean, empty, porcelain food dishes via an open entryway for 30 minutes. For PF training days (D2, D4, D9, D11, D16, D18, and D23 [F_2 only]), mice were provided 20 mg 5-TUL pellets in a nonporous, porcelain dish in the far right-hand corner of the PF-paired side. The 5-TUL pellets are similar in nutrient composition to the home cage diet but also contain sucrose to increase palatability. Mice were confined to the PF-paired side and allowed to consume the pellets for 30 minutes. The pellets were weighed immediately prior to and following the 30-minute session. For the no-PF training sessions (D3, D5, D10, D12, D17, and D19), mice were confined to the left side and provided a clean, empty porcelain dish. Control mice were presented with custom-designed chow-like pellets (20 mg; no sucrose) on the right side. We quantified the amount of food consumed as percent body weight (BW). Mice were assessed for PF conditioned place preference (CPP) on D8, D15, and D22 in the same manner as on D1. In panel **(A)**, D is day of protocol and CPP is day of CPP assessment. PF (20-mg pellets of 5-TUL diet) was provided on the right side for 30 minutes. For the no-PF session an empty dish was provided on the left side for 30 minutes. For the home cage session mice were left undisturbed in their home cage in the vivarium. **(B)** Dimensions and texture of the CPP apparatus. Time spent on the PF-paired side (right side) and time spent within the PF-paired triangle of the right side were examined. White circles denote the porcelain food bowls that contained food or no food. The two horizontal lines in the middle represent the entryway between each side that was open only during CPP assessment. **(C)** Assessment of B6 substrain differences in PF consumption (% BW) indicated a main effect of substrain ($F_{1,189}$ = 84.42, p = 2.0 × 10^{-16}) and a substrain × day interaction ($F_{6,189}$ = 3.45, p = .0028). B6NJ mice (n = 15; 8 female mice, 7 male mice) showed significantly greater PF consumption than did B6J mice (n = 8 female mice, 7 male mice) on D4–D23 ($t_{19–22}$ = 3.30–5.79, *p < .007; corrected .05 level for seven comparisons). The strain difference in summed PF consumed (% BW) across training days is shown in the inset (t_{21} = 4.73, p = .0001). **(D)** Slope analysis across PF training days indicated a steeper escalation in PF consumption in B6NJ vs. B6J mice ($F_{1,10}$ = 63.2, p < .0001). **(E)** For PF-CPP, there was no effect of strain ($F_{1,108}$ < 1), no effect of day ($F_{3,108}$ = 2.07, p = .11), and no interaction ($F_{3,108}$ = 1.04, p = .38). **(F)** When considering time spent in time spent in the PF triangle, there was no effect of substrain ($F_{1,108}$ < 1) and there was an effect of day ($F_{3,108}$ = 3.20, p = .03). **(G)** In considering differences in body weight between strains, there was no effect of strain ($F_{1,189}$ = 2.24, p = .14), no effect of day ($F_{6,189}$ < 1), and no interaction ($F_{6,189}$ < 1).

trained and tested for BE and PF-CPP on D1–D22. On D23, mice were provided 30-minute access to PF in the light side of the light/dark box and tested for compulsive-like eating. On D24, mice were sacrificed and striatum punches were harvested for RNA sequencing.

Transcriptome Analysis via RNA Sequencing

B6J × B6NJ-F_2 Study. A subset of PF-trained F_2 mice were chosen for transcriptome analysis that were homozygous for the wild-type B6J allele (BE resistant; $^{J/J}$) or the mutant B6NJ allele (BE prone; $^{N/N}$) at the *Cyfip2* missense mutation (rs240617401) and two flanking markers (rs48169870 and rs6268547) to ensure QTL capture. A sample size of $n = 8$ per genotype was employed (4 female mice, 4 male mice; 69–100 days old when sacrificed). Striatum punches were harvested on D24 following elevated plus maze testing, stored in RNAlater (Thermo Fisher Scientific, Waltham, MA) for 48 hours, blotted with a Kimwipe (Kimberly-Clark Professional, Roswell, GA), and transferred to −80°C. Total RNA was isolated (31,36) and shipped to the University of Chicago Genomics Core Facility (Chicago, IL) for complementary DNA library preparation and sequencing (31) (see Figure 4 legend and Supplement for additional details).

***Cyfip2*$^{N/-}$ Transcriptome Study.** On D24 (24 hours post light/dark test), mice were sacrificed and striatum punches were harvested and stored as described. We sequenced a subset of $n = 8$ mice per genotype (*Cyfip2*$^{N/N}$, *Cyfip2*$^{N/-}$) per treatment (PF, chow; 4 female mice, 4 male mice; 82–84 days old when sacrificed) that represented the group averages of compulsive-like eating. Samples were sequenced and analyzed similarly to F_2 mice. For most gene lists, we used a cutoff of greater than or equal to 1.1-fold change in expression (false discovery rate <20%). One exception was made for the small gene list derived from PF- versus chow-trained wild-type *Cyfip2*$^{N/N}$ mice where we employed a cutoff of $p < .0001$ (≥1.1-fold change). We chose a subset of genes for quantitative polymerase chain reaction validation (see below).

Enrichment Analysis

We applied Ingenuity Pathway Analysis (IPA) (www.qiagen.com/ingenuity) (37) to three gene lists: 1) F_2 mice (*Cyfip2*$^{N/N}$ vs. *Cyfip2*$^{J/J}$), 2) effect of genotype (*Cyfip2*$^{N/N}$ vs. *Cyfip2*$^{N/-}$), and 3) effect of treatment (PF vs. chow). We permitted 70 molecules per network and restricted assessment to neural tissues and cell lines. Statistical significance was assessed using Fisher's exact test with correction for multiple testing. We also used Enrichr (http://amp.pharm.mssm.edu/Enrichr/) to compute enrichment scores for ranked terms derived from 35 different gene set libraries. Finally, we used cell type-specific expression analysis (http://genetics.wustl.edu/jdlab/csea-tool-2/), which utilizes cell type-specific expression datasets to infer cell type enrichment (38).

RESULTS

BE and PF-CPP in B6 Substrains

The BE protocol and PF-CPP apparatus are shown in Figure 1A, B. Results from CFW mice in diet selection and the BE PF-CPP design are shown in Supplemental Figure S1 and Supplemental Table S1. CFW mice showed a robust escalation in PF consumption that correlated with PF-CPP for the 5-TUL diet (Supplemental Table S1). Because B6 substrains are an efficient tool for QTL mapping of complex behaviors induced by substances of abuse (29), we next tested for B6 substrain differences in the BE PF-CPP paradigm. We found robust differences in BE whereby B6NJ mice showed a greater and more rapid escalation of PF consumption than did B6J mice (Figure 1C, D) in the absence of any difference in PF-CPP (Figure 1E, F) or correlation with consumption (Supplemental Table S2). There were no strain differences in body weight during PF training (Figure 1G). Importantly, BE in binge-prone B6NJ mice was specific for PF because there was less initial and escalated intake with 20-mg chow pellets lacking sucrose (Supplemental Figure S2).

QTL Mapping in F_2 Mice

We next mapped the genetic basis of BE susceptibility in a B6J × B6NJ-F_2 cross. Supplemental Table S3 lists the single nucleotide polymorphism markers. We identified a single QTL on chromosome 11 for summed PF consumed that peaked at the *Cyfip2* missense mutation (46,222,615 bp; mm10, rs240617401; Figure 2A, B). The allelic effect was in the same phenotypic direction as the parental strains (*Cyfip2*$^{N/N}$ > *Cyfip2*$^{J/J}$), was consistent across D2–D16, and was less robust during later training days (D18–D23; Figure 2C, D).

We estimated environmental variance using phenotypic variance of B6J, B6NJ, and F_1 mice (Supplemental Figure S3) (29). The *Cyfip2* locus accounted for 16% of the phenotypic and 33% of the genetic variance. The estimated narrow-sense heritability of the QTL for total PF consumption was 49% (29). The QTL was more robust in female mice (Figure 2B, E, F) and peaked on D2. A second, distal QTL was identified in female mice on D9 and D11 (Figure 2E). In male mice, a single QTL was centered near *Cyfip2* but no individual day was significant (Figure 2G, H).

Female F_2 mice consumed more PF and escalated more rapidly than male mice (Supplemental Figure S4A, B) without any difference in PF-CPP (Supplemental Figure S4C, D). Female mice also showed an increase in freezing episodes in the elevated plus maze relative to male mice (Supplemental Figure S4E, F). No sex difference was observed in a separate cohort of F_2 mice that previously received saline injections during CPP (30) (Supplemental Figure S4G, H).

BE and Compulsive-Like Eating in *Cyfip2*$^{N/N}$ and *Cyfip2*$^{N/-}$ Mice

Because the QTL for PF consumption peaked near the *Cyfip2* missense mutation (*Cyfip2*$^{N/N}$) associated with cocaine behavior in B6 substrains (29) and because the mesocorticolimbic dopaminergic circuitry is crucial for BE (13), we hypothesized that *Cyfip2*$^{N/N}$ is a major genetic factor underlying BE. *Cyfip2*$^{N/-}$ mice (Supplemental Figure S5A) showed reduced PF consumption but not reduced chow consumption (Figure 3A, B) toward a wild-type B6J-like level (Figures 1C, 2D). No difference in CPP was observed (Supplemental Figure S5). Similar effects of genotype on BE were observed in female and male mice

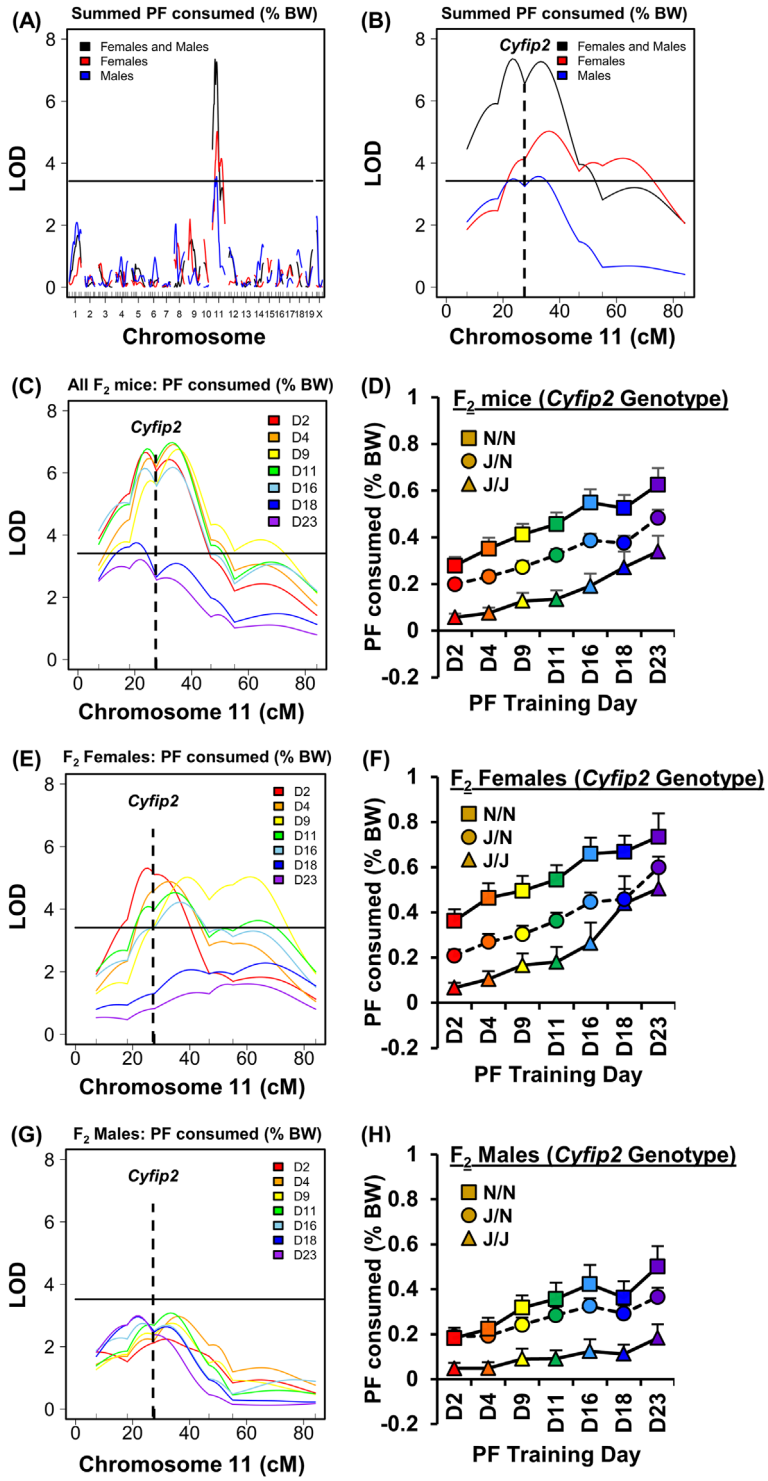

Figure 2. Quantitative trait loci (QTL) near *Cyfip2* on chromosome 11 in C57BL/6J (B6J) × C57BL/6NJ (B6NJ) F_2 mice. The F_2 dataset and R code for QTL analysis are available at GitHub (https://github.com/camronbryant/QTL_BingeEating_B6Substrains). The phenotype of B6J × B6NJ-F_1 mice (Supplemental Figure S3) vs. parental strains (Figure 1C, D) suggested that the B6NJ allele was semidominant (29). **(A, B)** A single genome-wide significant QTL for summed palatable food (PF) consumed (% body weight [BW]) was identified on chromosome 11 that peaked at the location of the *Cyfip2* missense mutation (rs240617401; 28 cM; 46,222,615 bp; mm10; logarithm of the odds (LOD) = 7.4; bolded uptick on x axis of QTL plots) previously identified for cocaine behavioral sensitivity (29). The 1.5 LOD support interval was defined by the nearest markers flanking the peak (rs48169870, rs13481117) and spanned 31 Mb-79 Mb. We considered female and male mice combined (black trace), female mice only (red trace), or male mice only (blue trace) in the analysis. The significance thresholds are represented by the horizontal lines, which were nearly identical for the three separate analyses and thus overlay one another. **(C, D)** The time course of the effect plot for the *Cyfip2* marker (rs240617401; bolded uptick) across PF training days indicated that the most significant LOD score and largest separation of genotypes in PF consumption occurred during the earlier training days (day [D] 2 to D11; red, orange, yellow, green, light blue). **(E, F)** For F_2 female mice (n = 78), the effect plot for the *Cyfip2* marker (bolded uptick on x axis) indicated that the QTL peaked early on D2 (red) and that a second more distally localized QTL emerged on D9 and D11 at 60 cM (green, yellow). Coding and structural variants on distal chromosome 11 identified via whole genome sequencing include an initiator codon variant in *Stxbp4* (syntaxin binding protein 4; 90 Mb) located at 90 Mb and an intronic, retrotransposon insertion in *Rptor* (regulatory associated protein of mechanistic target of rapamycin [mTOR] complex 1; 120 Mb) (26,42,72). **(G, H)** For F_2 male mice (n = 78), the QTL traces and effect plots indicated suggestive peaks located near *Cyfip2* (bolded uptick on x axis), none of which were genome-wide significant. Six missing genotypes at rs240617401 were imputed for QTL analysis **(A, C, E)**. The effect plots represent phenotypic data from the 150 of 156 called genotypes, including n = 33 $Cyfip2^{J/J}$ (16 female mice, 17 male mice), n = 85 $Cyfip2^{J/N}$ (43 female mice, 42 male mice), and n = 32 $Cyfip2^{N/N}$ (17 female mice, 15 male mice). Data are presented as the mean ± SEM. The significance thresholds (horizontal lines) in panels **(C)**, **(E)**, and **(G)** represent D2, which was the highest (most conservative) threshold across all days.

(Supplemental Figure S6); thus, we collapsed across sex for behavioral and transcriptome analyses. Slope analysis identified a greater y intercept in PF-trained $Cyfip2^{N/N}$ versus $Cyfip2^{N/-}$ mice (m = 0.173 vs. 0.063; $F_{1,11}$ = 18.1, p = .001). For chow groups, the slopes did not differ from zero ($p > .05$), indicating specificity for PF. Importantly, $Cyfip2^{N/-}$ mice showed reduced compulsive-like eating and concomitant behaviors relative to $Cyfip2^{N/N}$ mice (Figure 3C–F).

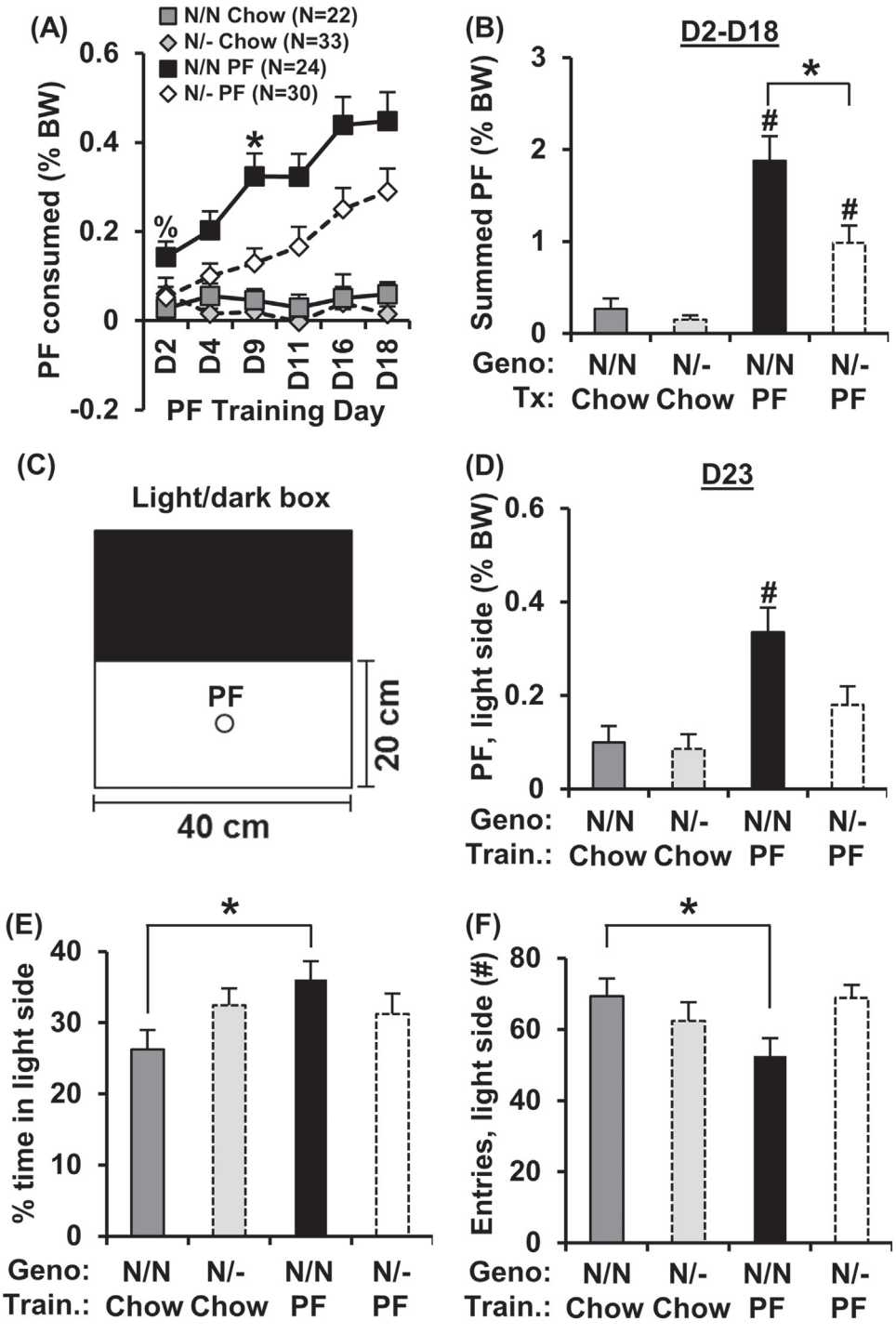

Figure 3. Reduced binge eating in *Cyfip2*$^{N/-}$ mice. **(A)** In examining changes in food consumption across days, there was an effect of genotype ($F_{1,623}$ = 42.45, p = 1.5 × 10^{-10}), treatment ($F_{1,623}$ = 181.4, p < 2.0 × 10^{-16}), a genotype × treatment interaction ($F_{5,623}$ = 19.59, p = 1.13 × 10^{-5}), and a treatment × day interaction ($F_{5,623}$ = 9.78, p = 5.25 × 10^{-9}). To reveal the source of the interactions, two-way analysis of variance for each day identified significant genotype × treatment interactions on day (D) 2, D9, and D16 ($F_{1,105}$ = 7.39, 6.76, 4.71, p = .007, 0.011, 0.032, respectively) that were in part explained by increased palatable food (PF) vs. chow consumption in *Cyfip2*$^{N/N}$ mice but not *Cyfip2*$^{N/-}$ mice on D2 (t_{50} = 3.11; $^{\%}p$ < .0125; Bonferroni corrected for four comparisons) and by increased PF consumption in *Cyfip2*$^{N/N}$ vs. *Cyfip2*$^{N/-}$ mice on D9 (t_{39} = 3.19, $^{*}p$ < .0125). No differences in chow pellet consumption were observed between *Cyfip2*$^{N/N}$ and *Cyfip2*$^{N/-}$ mice across any training day (p > .0125). **(B)** For total food consumption, there was an effect of genotype (Geno) ($F_{1,150}$ = 11.29, p = .001) and treatment (Tx) ($F_{1,105}$ = 49.87, p = 1.85 × 10^{-10}), and an interaction ($F_{1,105}$ = 5.35, p = .02). Both *Cyfip2*$^{N/N}$ and *Cyfip2*$^{N/-}$ mice showed greater PF consumption compared with their respective chow groups (t_{33} = 5.6, 4.32, $^{\#}p$ < .0125). Furthermore, *Cyfip2*$^{N/N}$ mice consumed more PF than did *Cyfip2*$^{N/-}$ mice (t_{43} = 2.75, $^{*}p$ < .0125), but did not consume more chow (t_{29} = 1.0, p > .0125). **(C)** Dimensions of light/dark conflict test of compulsive-like PF consumption provided in the center of the light side. **(D)** In measuring compulsive-like PF consumption in the light/dark conflict test, there was a main effect of genotype ($F_{1,105}$ = 14.83, p = .0002) and training treatment (Train.) ($F_{1,105}$ = 5.14, p = .025), but no interaction ($F_{1,105}$ = 3.06, p = .08). Only the PF-trained *Cyfip2*$^{N/N}$ mice consumed more PF than did their chow-trained *Cyfip2*$^{N/N}$ control mice ($^{\#}t_{39}$ = 3.68; p < .0125). There was no difference in PF consumption in chow-trained *Cyfip2*$^{N/N}$ vs. chow-trained *Cyfip2*$^{N/-}$ mice (t_{47} < 1), demonstrating a selective reduction of compulsive-like PF consumption in *Cyfip2*$^{N/-}$ mice. **(E, F)** In examining concomitant percent time on the light side and the number of entries into the light side during compulsive-like PF consumption, there were significant genotype × training treatment interactions ($F_{1,105}$ = 4.23, 5.48, p = .04, .02, respectively) that were explained by PF-trained *Cyfip2*$^{N/N}$ mice exhibiting an increase in time spent on the light side and a decrease in the number of entries to the light side relative to chow-trained *Cyfip2*$^{N/N}$ mice ($t_{38–43}$ = 2.67, 2.63, $^{*}p$ < .0125, respectively) whereas chow- vs. PF-trained *Cyfip2*$^{N/-}$ mice did not differ from their chow-trained *Cyfip2*$^{N/-}$ control mice ($t_{58–60}$ < 1). BW, body weight.

Transcriptome of Binge-Prone *Cyfip2*$^{N/N}$ F_2 Mice Versus Binge-Resistant *Cyfip2*$^{J/J}$ F_2 Mice

To gain insight into the neurobiological mechanisms that bridge *Cyfip2* polymorphisms with BE, we sequenced striatal RNA from a subset of binge-prone *Cyfip2*$^{N/N}$ and binge-resistant *Cyfip2*$^{J/J}$ F_2 mice based on D2 PF consumption (Supplemental Figure S7A), a phenotype with a highly significant QTL (Figure 2C, E). We obtained an average of 50 million reads per sample and identified 576 differentially expressed genes (338 downregulated genes, 238 upregulated genes with greater than or equal to 1.1-fold change [false discovery rate <0.2; Figure 4A and Supplemental Table S4]). The top GO terms were associated with synaptic components and plasticity, behavior, axonogenesis, ion channels, transporters, and glutamate receptors (Table 1A and Supplemental Table S11A). Top KEGG terms included endocannabinoid signaling, morphine addiction, and nicotine addiction as well as gamma-aminobutyric acidergic, glutamatergic, dopaminergic, and cholinergic synapses (Table 1A and Supplemental Table S11A).

Transcriptome Analysis of Compulsive-Like Eating in *Cyfip2*$^{N/N}$ and *Cyfip2*$^{N/-}$ Mice

Analysis of select F_2 mice (all PF trained) precluded us from isolating the effect of genotype versus treatment on the transcriptome. Thus, we examined the premorbid transcriptome (effect of genotype) and the transcriptome associated with compulsive-like eating (effect of treatment). Striatal messenger RNA was sequenced from a subset ($n = 8$) of representative mice from the four groups assayed for compulsive-like eating (Supplemental Figure S7B). We obtained an average of 45 million reads per sample and identified 224 genes for the main effect of genotype (Figure 4A and Supplemental Table S5) and 42 genes for the main effect of treatment (Figure 4A and Supplemental Table S6). Because only *Cyfip2*$^{N/N}$ mice showed compulsive-like eating, we also included differentially expressed genes between PF- versus chow-trained *Cyfip2*$^{N/N}$ mice ($p < .0001$) for a total of 61 genes in enrichment analysis of treatment (Figure 4A and Supplemental Tables S7, S8).

For the genotype $\times$ treatment interaction, we identified five genes (*Rn18s*, *Rn45s*, *Lars2*, *Glul*, *Gjb6*, and *Gstm5*). The behavioral interaction was driven by compulsive-like eating in *Cyfip2*$^{N/N}$ mice (Figure 3D); thus, we also examined pairwise differential gene expression between PF-trained *Cyfip2*$^{N/-}$ versus *Cyfip2*$^{N/N}$ mice (Supplemental Table S9) and identified 44 unique genes (Supplemental Table S10; see IPA network in Supplemental Figure S9).

For the effect of genotype, there was extensive overlap with the F_2 gene list (Figure 4A). Importantly, the direction and degree of differential expression in the *Cyfip2*$^{N/N}$ genotype versus the *Cyfip2*$^{J/J}$ or *Cyfip2*$^{N/-}$ genotype were highly correlated Figure 4B), indicating that like behavior, *Cyfip2*$^{J/J}$ and *Cyfip2*$^{N/-}$ alleles induced functionally similar effects on gene transcription relative to *Cyfip2*$^{N/N}$. This correlation was not driven by the fold-change cutoff (Supplemental Figure S8).

Enrichment analysis for the effect of genotype (*Cyfip2*$^{N/-}$ relative to *Cyfip2*$^{N/N}$) identified GO terms in Table 1B (see also Supplemental Table S11B). Top canonical IPA pathways included G protein, cyclic adenosine monophosphate, G protein–coupled receptor, and gamma-aminobutyric acid receptor signaling (-logP = 4.72–9.34). Top upstream regulators included *Htt*, L-dopa, ciliary neurotrophic factor, *Foxp1*, and ethanol ($p = 1.46 \times 10^{-12}$ to 1.46×10^{-6}). Notably, ciliary neurotrophic factor treatment can suppress food intake, induce weight and fat loss, and improve metabolic syndrome (39) and was associated in binge-resistant *Cyfip2*$^{N/-}$ mice with downregulation of *Chat*, *Drd2*, *Pde1b*, *Penk*, *Ppp1r1b*, and *Tac1* and upregulation of *Vip* (Supplemental Table S5). The top IPA network was behavior, endocrine system development and function, molecular transport where dopamine was an enriched IPA molecule for *Ppp1r1b* (DARPP-32), *Drd2*, *Penk*, *Chrm4*, *Gpr22*, *Adcy5*, *Kcnab3*, *Pde1b*, and *Hrh3* (Figure 4C). Finally, cell type-specific expression analysis identified the highest enrichment for genes in D1 and D2 striatal spiny neurons (Figure 4E).

For the effect of treatment (PF relative to chow), GO terms are listed in Table 1C (see also Supplemental Table S11C). *Tcf7l2* (T-cell specific, high-mobility group box) was the top IPA upstream regulator ($p = 1.09 \times 10^{-23}$) with 21 downregulated genes (see the transcription factor 7-like 2 node in Figure 4D). Transcription factor 7-like 2 is a transcription factor that regulates peptide secretion and is associated with type 2 diabetes, dietary preference, obesity, blood glucose homeostasis, metabolic syndrome, and BE in bipolar disorder (40,41). The top IPA network for treatment included 30 downregulated genes enriched for cellular development, nervous system development and function, tissue morphology (Figure 4D). Strikingly, most of these genes were enriched for myelination, axon ensheathment, glial cell, and oligodendrocyte formation and differentiation (Table 1C and Supplemental Table S11C). None of these genes were identified in binge-resistant *Cyfip2*$^{N/-}$ mice or from the effect of genotype (Figure 4A), indicating specificity for BE. In support, cell type-specific expression analysis identified an enrichment of genes in oligodendrocytes and progenitors (Figure 4F). Thus, the transcriptional profile of BE implicates decreased oligodendrocytes and myelination as a neurobiological consequence of BE. We validated a subset of genes for the effect of genotype and treatment via quantitative polymerase chain reaction (Supplemental Tables S12 and S13, Supplemental Figure S10).

DISCUSSION

We exploited the large phenotypic and small genetic diversity of B6 substrains to identify *Cyfip2* as a major genetic factor underlying BE (Figures 1–3). Our study was facilitated by whole genome sequencing of B6 substrains (26,29,42) and the identification of the same locus and gene associated with psychostimulant-induced neurobehavioral plasticity (29). The difference in direction of the effect of the *Cyfip2*$^{N/N}$ allele on BE (increase) versus psychostimulant behavior (decrease) could potentially indicate differences in underlying neurobiological mechanisms. However, it should be noted that the cocaine results were obtained from experimenter-delivered drug administration whereas the BE results were obtained from voluntary PF consumption.

Several observations suggest that *Cyfip2* is associated with the immediate consummatory response to PF that drives BE behavior. First, B6 substrain differences in PF-CPP were not

significant (Figure 1E, F). Second, there was no correlation between consumption and PF-CPP in F_2 mice (Supplemental Table S2). Third, no significant QTL for PF-CPP was identified. Fourth, there was no effect of the *Cyfip2*$^{N/-}$ allele on PF-CPP (Supplemental Figure S5). Finally, the largest effect of the *Cyfip2* locus on PF consumption was observed on D2 (Figure 2E).

The *Cyfip2*$^{N/N}$ allele is associated with decreased protein stability (29), which represents just one molecular correlate associated with this mutation. If considered in isolation, a

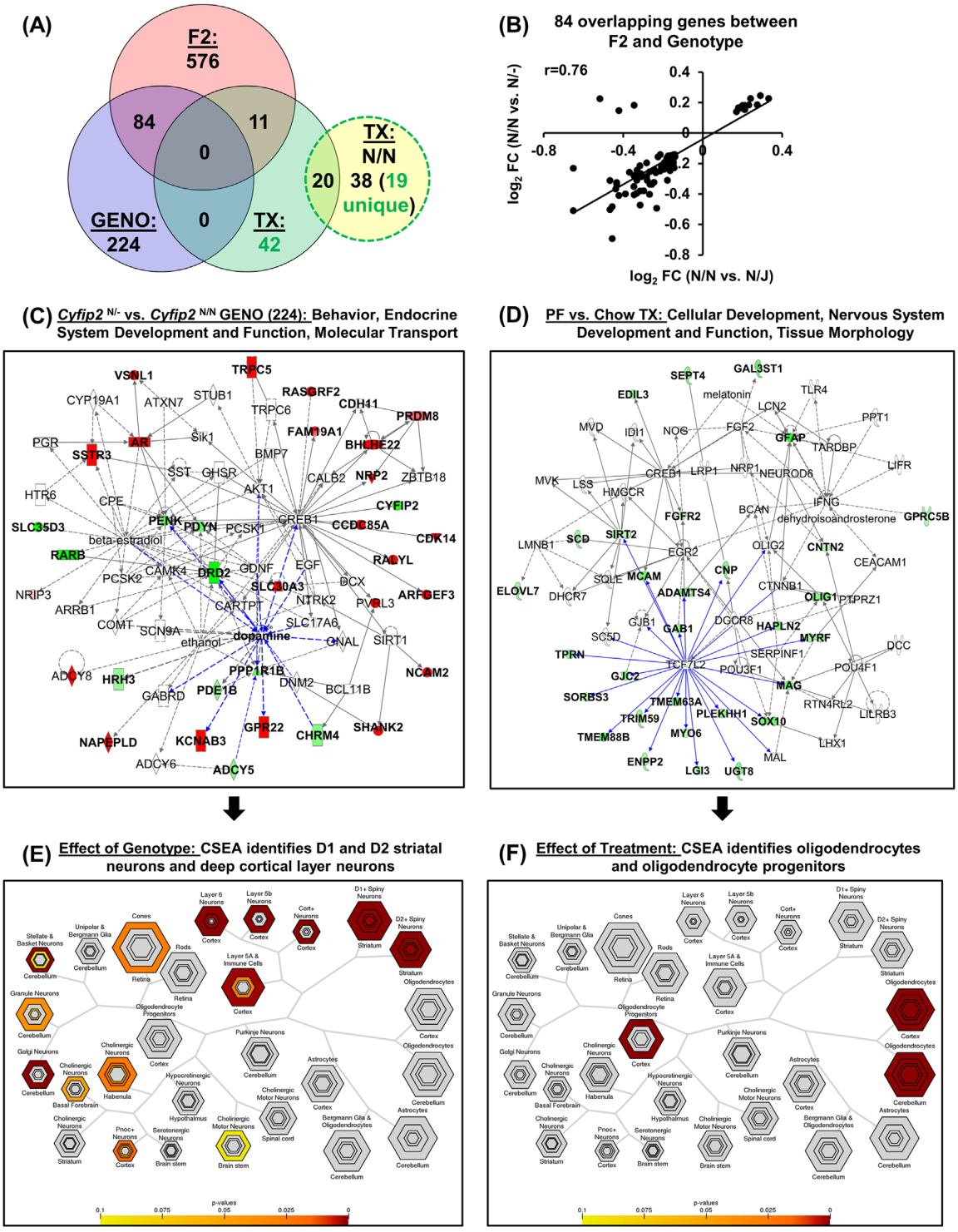

decrease in protein stability suggests a loss-of-function and the predicted phenotype should be similar to the *Cyfip2*$^{N/-}$ allele. However, *Cyfip2*$^{N/N}$ codes for a S968F missense mutation (29) that is translated and could modulate other molecular functions (protein-protein interactions) to affect neural development and behavior.

The *Cyfip2*$^{N/N}$ mutation was associated with decreased cocaine-induced locomotor stimulation, dendritic spine number, and glutamatergic neurotransmission in the nucleus accumbens that were partially reversed in *Cyfip2*$^{N/-}$ mice toward a *Cyfip2*$^{J/J}$-like level (29). The BE phenotype and the transcriptome of *Cyfip2*$^{N/N}$ mice were also partially reversed in *Cyfip2*$^{N/-}$ mice toward a *Cyfip2*$^{J/J}$-like level (Figures 3, 4B). Enrichment analysis of *Cyfip2*$^{N/-}$ versus *Cyfip2*$^{N/N}$ genotypes identified channel regulator activity, glutamate receptor binding, and ionotropic glutamate receptor binding as the top three molecular GO terms and glutamatergic synapse as the top KEGG term (Table 1B and Supplemental Table S11B). Interestingly, the glutamatergic system may be an effective target for BE (43,44). Cytoplasmic FMR1 interacting protein (CYFIP) 1/2 is a component of the Wiskott-Aldrich syndrome protein family verprolin-homologous protein regulatory complex (45) and also associates with fragile X mental retardation protein (46). Both Wiskott-Aldrich syndrome protein family verprolin-homologous protein (WAVE) and fragile X mental retardation protein regulate dendritic spine morphology and synaptic plasticity (45,47). CYFIP modulates protein interactions in the FMRP-ribosome complex (48) to regulate activity-dependent synaptic translation and plasticity. In addition to glutatmatergic transmission, the premorbid *Cyfip2* genotype also perturbed gene sets enriched for the KEGG terms morphine addiction and retrograde endocannabinoid signaling (Table 1B). The overlap of these top enrichment terms in two independent transcriptome studies (Table 1A, B) provided additional support that premorbid differential gene expression within these gene sets could bridge *Cyfip2* genotype with susceptibility to BE.

Female F_2 mice were more prone to BE (Figure 2 and Supplemental Figure S4A, B) (49–51) which is consistent with human studies (52) and could potentially be explained by the sweetened PF diet (51,53), neurodevelopmental sex differences in the food reward circuitry and response to PF (54), activational effects of gonadal steroids (50,52,55), impulsivity (56), and/or neurobehavioral plasticity that underlies negative reinforcement (57). We did not observe sex differences in PF-CPP in F_2 mice (Supplemental Figure S4C, D); however, we did observe an increase in freezing episodes in female F_2 mice at 24 hours post-BE that was specific to PF training (Supplemental Figure S4F–H). We previously observed an increase in freezing episodes in a place-conditioning paradigm that correlated with conditioned place aversion induced by blockade of endogenous opioid signaling (30).

Cyfip2$^{N/-}$ mice showed reduced compulsive-like eating compared with *Cyfip2*$^{N/N}$ mice as indicated by decreased PF consumption on the light side (Figure 3)—an aversive, bright environment that mice normally avoid. Compulsive-like PF consumption was associated with a downregulation of a large set of myelination genes in the striatum (Table 1C, Supplemental Table S11C and Figure 4D). Brain imaging studies in patients with bulimia nervosa found a reduction in white matter integrity in pathways linking frontal and temporoparietal cortices and limbic regions, including the fornix, internal capsule, corpus callosum, subinsula, and corona radiata (58,59). Furthermore, loss of white matter integrity correlated with the number of BE episodes (58), indicating a potential link between reduced myelination and increased symptomatic severity. White matter pathology was also observed in the brains of anorexic patients exhibiting restricted food intake (60,61). Furthermore, rodents restrict chow intake between intermittent binge episodes of limited access to PF (62–64). Thus, although we did not measure home cage chow intake, the reduced expression of myelination genes could ultimately be caused by repeated cycles of

Figure 4. Effect of genotype and treatment on the striatal transcriptome. The F_2 dataset is available on Gene Expression Omnibus (http://www.ncbi.nlm.nih.gov/geo/query/acc.cgi?token=kdcviyasnvmxfen&acc=GSE84252). The dataset for *Cyfip2*$^{N/N}$ and *Cyfip2*$^{N/-}$ mice is available at Gene Expression Omnibus (http://www.ncbi.nlm.nih.gov/geo/query/acc.cgi?token=ixixoekcdrcxtqt&acc=GSE84329). **(A)** Venn diagram indicates the number of differentially expressed genes and their overlap between F_2 vs. knockout analysis from the main effect of *Cyfip2* genotype (GENO) (*Cyfip2*$^{N/-}$ vs. *Cyfip2*$^{N/N}$) or treatment (TX) (palatable food [PF] vs. chow). A total of 224 genes from the main effect of GENO and 61 unique genes from the main effect of TX (green-colored numbers) were included in subsequent enrichment analyses. **(B)** Correlation of $\log_2$ fold-change (FC) in gene expression from the 84 overlapping genes identified in *Cyfip2*$^{N/N}$ mice from the F_2 study (relative to *Cyfip2*$^{J/J}$; x axis) vs. the knockout study (relative to *Cyfip2*$^{N/-}$; y axis; $r = .76$, $r^2 = .58$; $F_{1,82} = 115.2$, $p = 2.7 \times 10^{-17}$). **(C)** The top Ingenuity Pathway Analysis network for the effect of GENO is shown (enrichment score = 36). Green = downregulated in binge-resistant *Cyfip2*$^{N/-}$ mice (or, i.e., upregulated in binge-susceptible *Cyfip2*$^{N/N}$ mice). Red = upregulated in binge-resistant *Cyfip2*$^{N/-}$ mice (or, i.e., downregulated in binge-susceptible *Cyfip2*$^{N/N}$ mice). **(D)** The top Ingenuity Pathway Analysis network for the effect of treatment is shown (enrichment score = 28). Green = downregulated in PF-trained mice. **(E, F)** Cell type-specific expression analysis (CSEA) results for the effect of **(E)** genotype or **(F)** treatment are presented as bullseye plots for each cell type. The topographical plot represents the hierarchical clustering of each cell type based on the relative gene expression profile (38). The specificity index probability statistic (73) was previously used to identify cell-specific reference gene lists that were used to build the bullseye plots. The size of the hexagon for each cell type is scaled to the number of transcripts expressed in that particular cell type relative to the other cell types. The bullseye plot is divided into four separate rings. The outer ring represents the reference gene set with the least stringent threshold of enrichment for that particular cell type ($p < .05$) whereas the inner ring (the bullseye) represents the reference gene set with the most stringent threshold of enrichment for that particular cell type ($p < 1 \times 10^{-4}$). The degree of enrichment of one's own experimentally derived gene list for the reference gene list within each ring is color coded based on the p value derived from a Fisher's exact test. Enrichment signals originating from the outer rings are more likely to contain genes that are somewhat more promiscuously expressed across different cell types whereas enrichment signals located at the center bullseye represent genes that are the most exclusive for that particular cell type (38). **(E)** For the effect of genotype, only D_1 and D_2 striatal spiny neurons contained a strong enrichment signal within all rings of the two cell types (including the bullseye), which indicates an enrichment for gene sets that are most exclusive for D1 and D2 striatal spiny neurons. In contrast, only the outer rings of other cell types contained enrichment signals (cortical, cerebellar, cholinergic, and serotonergic neurons and cones) which are more likely to be driven by somewhat more promiscuously expressed genes across different cell types. Enrichment in deep cortical layers could also reflect an imprecision in the dissection punches. **(F)** For the effect of treatment, the enrichment signals were exclusive to oligodendrocyte progenitors and oligodendrocytes.

Table 1. Enrichment Analyses of Binge-Prone *Cyfip2*$^{N/N}$ F_2 Mice vs. Binge-Resistant *Cyfip2*$^{J/J}$ F_2 Mice, the Effect of Genotype (*Cyfip2*$^{N/-}$ Mice vs. *Cyfip2*$^{N/N}$ Mice), and the Effect of Treatment (PF vs. Chow)

	Term	Overlap	*p*	FDR
A: Binge-Prone *Cyfip2*$^{N/N}$ F_2 Mice vs. Binge-Resistant *Cyfip2*$^{J/J}$ F_2 Mice				
GO: Biological process				
GO: 0007268	Synaptic transmission	60/434	7.5E-21	2.4E-17
GO: 0007610	Behavior	49/494	4.1E-12	6.5E-09
GO: 0032940	Secretion by cell	41/415	2.9E-10	3.1E-07
GO: 0007626	Locomotory behavior	25/183	3.2E-09	2.6E-06
GO: 0044708	Single-organism behavior	35/362	1.0E-08	6.6E-06
GO: Cellular component				
GO: 0044456	Synapse part	42/395	1.9E-11	6.2E-09
GO: 0034702	Ion channel complex	31/258	6.5E-10	1.1E-07
GO: 1902495	Transmembrane transporter complex	31/286	6.2E-09	6.8E-07
GO: 1990351	Transporter complex	31/291	9.0E-09	7.4E-07
GO: 0030425	Dendrite	27/236	2.2E-08	1.4E-06
GO: Molecular component				
GO: 0022836	Gated channel activity	31/323	3.3E-07	2.2E-04
GO: 0015267	Channel activity	35/427	1.8E-06	3.9E-04
GO: 0022803	Passive transmembrane transporter activity	35/427	1.8E-06	3.9E-04
GO: 0005216	Ion channel activity	33/396	2.6E-06	4.2E-04
GO: 0022838	Substrate-specific channel activity	33/406	4.2E-06	5.6E-04
KEGG ID				
hsa04723	Retrograde endocannabinoid signaling	21/101	1.1E-10	2.6E-08
hsa04727	Gamma-aminobutyric acidergic synapse	19/88	5.2E-10	6.0E-08
hsa05032	Morphine addiction	18/91	5.1E-09	3.9E-07
hsa04724	Glutamatergic synapse	19/114	2.2E-08	1.3E-06
hsa04713	Circadian entrainment	17/95	5.1E-08	2.4E-06
B: Effect of Genotype (*Cyfip2*$^{N/-}$ Mice vs. *Cyfip2*$^{N/N}$ Mice)				
GO: Biological process				
GO: 0007610	Behavior	31/494	1.3E-14	1.3E-11
GO: 0044708	Single-organism behavior	27/362	1.6E-14	1.3E-11
GO: 0007268	Synaptic transmission	29/434	2.2E-14	1.3E-11
GO: 0030534	Adult behavior	14/141	1.7E-09	7.3E-07
GO: 0007626	Locomotory behavior	15/183	4.9E-09	1.7E-06
GO: Cellular component				
GO: 0044456	Synapse part	23/395	1.4E-10	2.9E-08
GO: 0043025	Neuronal cell body	16/270	8.9E-08	8.5E-06
GO: 0044297	Cell body	17/315	1.2E-07	8.5E-06
GO: 0005887	Integral component of plasma membrane	30/1066	2.1E-06	9.4E-05
GO: 0097060	Synaptic membrane	13/228	2.3E-06	9.4E-05
GO: Molecular component				
GO: 0016247	Channel regulator activity	8/102	3.3E-05	6.5E-03
GO: 0035254	Glutamate receptor binding	5/29	3.6E-05	6.5E-03
GO: 0035255	Ionotropic glutamate receptor binding	4/17	7.9E-05	7.5E-03
GO: 0005249	Voltage-gated potassium channel activity	7/86	8.3E-05	7.5E-03
GO: 0004714	Transmembrane receptor protein tyrosine kinase activity	6/65	1.4E-04	1.0E-02
KEGG ID				
hsa04724	Glutamatergic synapse	13/114	3.1E-10	4.2E-08
hsa05032	Morphine addiction	11/91	4.7E-09	3.2E-07
hsa04723	Retrograde endocannabinoid signaling	11/101	1.3E-08	5.8E-07
hsa04725	Cholinergic synapse	10/111	3.2E-07	8.8E-06
hsa05030	Cocaine addiction	8/49	8.5E-08	2.9E-06

Table 1. Continued

	Term	Overlap	*p*	FDR
C: Effect of Treatment (PF vs. Chow)				
GO: Biological process				
GO: 0042552	Myelination	6/59	6.4E-08	2.6E-05
GO: 0008366	Axon ensheathment	6/62	8.5E-08	2.6E-05
GO: 0007272	Ensheathment of neurons	6/62	8.5E-08	2.6E-05
GO: 0021762	Substantia nigra development	4/45	1.9E-05	4.5E-03
GO: 0010001	Glial cell differentiation	4/61	6.0E-05	9.8E-03
GO: Cellular component				
GO:0043209	Myelin sheath	3/17	3.7E-05	4.1E-03
GO:0005902	Microvillus	4/61	6.1E-05	4.1E-03
GO:0097386	Glial cell projection	2/9	5.8E-04	1.9E-02
GO:0044224	Juxtaparanode region of axon	2/9	5.8E-04	1.9E-02
GO:0033270	Paranode region of axon	2/11	8.2E-04	2.1E-02
MGI: Mammalian phenotype 4				
MP0000920	Abnormal myelination	9/134	3.6E-10	8.6E-08
MP0002882	Abnormal neuron morphology	14/1006	8.3E-07	9.9E-05
MP0003634	Abnormal glial cell	7/231	7.2E-06	5.7E-04
MP0002066	Abnormal motor capabilities	14/1482	7.4E-05	4.4E-03
MP0000762	Abnormal tongue morphology	4/77	1.1E-04	5.4E-03

FDR, false discovery rate; PF, palatable food.

self-induced food restriction of home cage chow. Future studies will assess myelin-associated protein levels during binge withdrawal versus the binge-sated state to determine the persistence of the proposed decrease in myelination. Directly targeting oligodendrocytes in preclinical models will reveal the potential role of demyelination versus remyelination in development versus recovery from BE and could represent a new therapeutic avenue for ED.

Previous studies reported B6 substrain differences in weight gain from PF diets (65). A recent study using an N_2 cross found weak evidence for an association of a single nucleotide polymorphism near *Cyfip2* (rs13481014; chr. 11, 48 Mb) with high fat diet-induced obesity and lower leptin levels (66). Our BE procedure did not induce weight gain and there were no strain differences in body weight (Figure 1G). However, the differences in BE suggest that the *Cyfip2* locus could be associated with diet-induced obesity and metabolic dysfunction in B6 substrains under conditions of prolonged PF access that induce weight gain (66,67).

It is worth noting that *CYFIP1* (homolog of *CYFIP2*; 88% similarity in amino acid sequence) is deleted or imprinted in patients with type I Prader-Willi syndrome, a neurodevelopmental disorder defined by extreme hyperphagia (68) and a hyperresponsive reward system to food-associated cues (69). Type I deletions comprise 40% of Prader-Willi syndrome deletions and can be associated with more severe neurobehavioral pathology, including an increase in compulsive behavior (70,71). Based on our identification of *Cyfip2* for BE (Figure 3), the shared neurobiological function of CYFIP proteins (47) and the association of *CYFIP1* with Prader-Willi syndrome, one hypothesis is that *CYFIP1* polymorphisms also affect BE and hyperphagia.

We did not observe any genotype × sex interactions in behavior with our sample sizes and the effects of the *Cyfip2* locus (F_2 study) and genotype (knockout study) on behavior were similar between female and male mice. Combining sexes clearly improved our power to detect the *Cyfip2* QTL (Figure 2A, B) and changes in the transcriptome. Future studies in additional crosses should be powered to detect sex-specific QTL and genotype × sex interactions in BE that likely exist in genetically more complex populations. Furthermore, because our transcriptome analysis was limited by the number of samples, brain regions, cell types, and time points that could be examined, a comprehensive transcriptomic study of BE is warranted to further our understanding of the dynamic neurobiological mechanisms influencing susceptibility versus establishment and persistence of BE.

We identified *Cyfip2* as a major genetic factor in preclinical BE. These results suggest that *CYFIP2* and possibly *CYFIP1* could be associated with maladaptive feeding in humans. Our success in QTL mapping and gene validation provides a clear rationale for expanding QTL mapping studies of BE to genetically diverse rodent populations and reference panels. These efforts will inform human genome-wide association studies of ED and could reveal new therapeutic directions to pursue.

ACKNOWLEDGMENTS AND DISCLOSURES

This study was supported by National Institutes of Health/National Institute on Drug Abuse (NIH/NIDA) Grant Nos. R21DA038738 (to CDB), R03DA038287 (to CDB), R00DA029635 (to CDB), F31DA40324 (to NY), and R01DA030425 (to PC); NIH/National Institute of General Medical Sciences (NIGMS) for Grant No. T32GM008541 (to LRG, NY, and AFB); the Burroughs Wellcome Fund Transformative Training Program in Addiction Science Grant No. 1011479 (to NY and JW); and Boston University's Undergraduate Research Opportunities Program.

We thank Dr. Kenneth Albrecht and Gregory Martin at the Boston University Transgenic and Genome Engineering Core Facility for assistance in rederivation of *Cyfip2*$^{N/-}$ mice. We thank Dr. Joseph Dougherty for his advice on cell type-specific expression analysis.

The authors declare no biomedical financial interests or potential conflicts of interest.

ARTICLE INFORMATION

From the Laboratory of Addiction Genetics (SLK, LRG, NY, RKB, JW, ERR, AFB, KIL, KPL, CDB) and Laboratory of Addictive Disorders (PC), Department of Pharmacology and Experimental Therapeutics and Department of Psychiatry; Graduate Program in Biomolecular Pharmacology (LRG, NY, AFB); Ph.D. Program in Biomedical Sciences (JW), Graduate Program in Genetics and Genomics; Computational Biomedicine (DFJ, EJ); and Department of Psychiatry (KSM), Boston University School of Medicine; Transformative Training Program in Addiction Science (NY, JW) and Ph.D. Program in Bioinformatics (ERR, DFJ), Boston University, Boston, Massachusetts; The Jackson Laboratory (VK), Bar Harbor, Maine; and the Department of Anatomy and Neurobiology (MKM), University of Tennessee Health Science Center, Memphis, Tennessee.

Address correspondence to Camron D. Bryant, Ph.D., Laboratory of Addiction Genetics, Department of Pharmacology and Experimental Therapeutics and Department of Psychiatry, 72 E Concord St, L-606C, Boston, MA 02118; E-mail: camron@bu.edu.

Received Aug 4, 2016; revised Sep 14, 2016; accepted Oct 4, 2016.

Supplementary material cited in this article is available online at http://dx.doi.org/10.1016/j.biopsych.2016.10.021.

REFERENCES

1. Hudson JI, Hiripi E, Pope HG Jr., Kessler RC (2007): The prevalence and correlates of eating disorders in the National Comorbidity Survey Replication. Biol Psychiatry 61:348–358.
2. Smink FR, van Hoeken D, Hoek HW (2012): Epidemiology of eating disorders: Incidence, prevalence and mortality rates. Curr Psychiatry Rep 14:406–414.
3. Mazzeo SE, Bulik CM (2009): Environmental and genetic risk factors for eating disorders: What the clinician needs to know. Child Adolesc Psychiatr Clin N Am 18:67–82.
4. Boraska V, Franklin CS, Floyd JA, Thornton LM, Huckins LM, Southam L, *et al*. (2014): A genome-wide association study of anorexia nervosa. Mol Psychiatry 19:1085–1094.
5. Mitchell KS, Neale MC, Bulik CM, Aggen SH, Kendler KS, Mazzeo SE (2010): Binge eating disorder: A symptom-level investigation of genetic and environmental influences on liability. Psychol Med 40:1899–1906.
6. Bulik CM, Sullivan PF, Kendler KS (1998): Heritability of binge-eating and broadly defined bulimia nervosa. Biol Psychiatry 44:1210–1218.
7. Eddy KT, Keel PK, Dorer DJ, Delinsky SS, Franko DL, Herzog DB (2002): Longitudinal comparison of anorexia nervosa subtypes. Int J Eat Disord 31:191–201.
8. Bulik CM, Hebebrand J, Keski-Rahkonen A, Klump KL, Reichborn-Kjennerud T, Mazzeo SE, *et al*. (2007): Genetic epidemiology, endophenotypes, and eating disorder classification. Int J Eat Disord 40 (suppl):S52–S60.
9. Kaye WH, Bulik CM, Thornton L, Barbarich N, Masters K (2004): Comorbidity of anxiety disorders with anorexia and bulimia nervosa. Am J Psychiatry 161:2215–2221.
10. Smith DG, Robbins TW (2013): The neurobiological underpinnings of obesity and binge eating: A rationale for adopting the food addiction model. Biol Psychiatry 73:804–810.
11. Carlier N, Marshe VS, Cmorejova J, Davis C, Muller DJ (2015): Genetic similarities between compulsive overeating and addiction phenotypes: A case for "food addiction"? Curr Psychiatry Rep 17:96.
12. Schulte EM, Grilo CM, Gearhardt AN (2016): Shared and unique mechanisms underlying binge eating disorder and addictive disorders. Clin Psychol Rev 44:125–139.
13. Bello NT, Hajnal A (2010): Dopamine and binge eating behaviors. Pharmacol Biochem Behav 97:25–33.
14. Giuliano C, Cottone P (2015): The role of the opioid system in binge eating disorder. CNS Spectr 20:537–545.
15. Sobik L, Hutchison K, Craighead L (2005): Cue-elicited craving for food: A fresh approach to the study of binge eating. Appetite 44:253–261.
16. Wang GJ, Geliebter A, Volkow ND, Telang FW, Logan J, Jayne MC, *et al*. (2011): Enhanced striatal dopamine release during food stimulation in binge eating disorder. Obesity (Silver Spring) 19:1601–1608.
17. Tomasi D, Volkow ND (2013): Striatocortical pathway dysfunction in addiction and obesity: Differences and similarities. Crit Rev Biochem Mol Biol 48:1–19.
18. Tellez LA, Han W, Zhang X, Ferreira TL, Perez IO, Shammah-Lagnado SJ, *et al*. (2016): Separate circuitries encode the hedonic and nutritional values of sugar. Nat Neurosci 19:465–470.
19. DiFeliceantonio AG, Mabrouk OS, Kennedy RT, Berridge KC (2012): Enkephalin surges in dorsal neostriatum as a signal to eat. Curr Biol 22:1918–1924.
20. Lawrence AD (2012): Affective neuroscience: Food 'wanting' hotspot in dorsal striatum. Curr Biol 22:R878–R880.
21. Frank GK, Shott ME, Hagman JO, Mittal VA (2013): Alterations in brain structures related to taste reward circuitry in ill and recovered anorexia nervosa and in bulimia nervosa. Am J Psychiatry 170:1152–1160.
22. Everitt BJ, Robbins TW (2013): From the ventral to the dorsal striatum: Devolving views of their roles in drug addiction. Neurosci Biobehav Rev 37:1946–1954.
23. Kas MJ, Kaye WH, Foulds Mathes W, Bulik CM (2009): Interspecies genetics of eating disorder traits. Am J Med Genet B Neuropsychiatr Genet 150B:318–327.
24. Bulik CM, Bacanu SA, Klump KL, Fichter MM, Halmi KA, Keel P, *et al*. (2005): Selection of eating-disorder phenotypes for linkage analysis. Am J Med Genet B Neuropsychiatr Genet 139B:81–87.
25. Bacanu SA, Bulik CM, Klump KL, Fichter MM, Halmi KA, Keel P, *et al*. (2005): Linkage analysis of anorexia and bulimia nervosa cohorts using selected behavioral phenotypes as quantitative traits or covariates. Am J Med Genet B Neuropsychiatr Genet 139B:61–68.
26. Keane TM, Goodstadt L, Danecek P, White MA, Wong K, Yalcin B, *et al*. (2011): Mouse genomic variation and its effect on phenotypes and gene regulation. Nature 477:289–294.
27. Bryant CD (2011): The blessings and curses of C57BL/6 substrains in mouse genetic studies. Ann N Y Acad Sci 1245:31–33.
28. Bryant CD, Zhang NN, Sokoloff G, Fanselow MS, Ennes HS, Palmer AA, *et al*. (2008): Behavioral differences among C57BL/6 substrains: Implications for transgenic and knockout studies. J Neurogenet 22: 315–331.
29. Kumar V, Kim K, Joseph C, Kourrich S, Yoo SH, Huang HC, *et al*. (2013): C57BL/6N mutation in cytoplasmic FMRP interacting protein 2 regulates cocaine response. Science 342:1508–1512.
30. Kirkpatrick SL, Bryant CD (2015): Behavioral architecture of opioid reward and aversion in C57BL/6 substrains. Front Behav Neurosci 8: 450.
31. Yazdani N, Parker CC, Shen Y, Reed ER, Guido MA, Kole LA, *et al*. (2015): Hnrnph1 is a quantitative trait gene for methamphetamine sensitivity. PLoS Genet 11:e1005713.
32. Cottone P, Wang X, Park JW, Valenza M, Blasio A, Kwak J, *et al*. (2012): Antagonism of sigma-1 receptors blocks compulsive-like eating. Neuropsychopharmacology 37:2593–2604.
33. Babbs RK, Wojnicki FH, Corwin RL (2012): Assessing binge eating. An analysis of data previously collected in bingeing rats. Appetite 59: 478–482.
34. Broman KW, Wu H, Sen S, Churchill GA (2003): R/qtl: QTL mapping in experimental crosses. Bioinformatics 19:889–890.
35. Cox A, Ackert-Bicknell CL, Dumont BL, Ding Y, Bell JT, Brockmann GA, *et al*. (2009): A new standard genetic map for the laboratory mouse. Genetics 182:1335–1344.
36. Bryant CD, Kole LA, Guido MA, Sokoloff G, Palmer AA (2012): Congenic dissection of a major QTL for methamphetamine sensitivity implicates epistasis. Genes Brain Behav 11:623–632.
37. Kramer A, Green J, Pollard J Jr., Tugendreich S (2014): Causal analysis approaches in ingenuity pathway analysis. Bioinformatics 30: 523–530.
38. Xu X, Wells AB, O'Brien DR, Nehorai A, Dougherty JD (2014): Cell type-specific expression analysis to identify putative cellular mechanisms for neurogenetic disorders. J Neurosci 34:1420–1431.
39. Pasquin S, Sharma M, Gauchat JF (2015): Ciliary neurotrophic factor (CNTF): New facets of an old molecule for treating neurodegenerative and metabolic syndrome pathologies. Cytokine Growth Factor Rev 26:507–515.

40. Cuellar-Barboza AB, Winham SJ, McElroy SL, Geske JR, Jenkins GD, Colby CL, *et al*. (2016): Accumulating evidence for a role of TCF7L2 variants in bipolar disorder with elevated body mass index. Bipolar Disord 18:124–135.
41. Winham SJ, Cuellar-Barboza AB, Oliveros A, McElroy SL, Crow S, Colby C, *et al*. (2014): Genome-wide association study of bipolar disorder accounting for effect of body mass index identifies a new risk allele in TCF7L2. Mol Psychiatry 19:1010–1016.
42. Simon MM, Greenaway S, White JK, Fuchs H, Gailus-Durner V, Sorg T, *et al*. (2013): A comparative phenotypic and genomic analysis of C57BL/6J and C57BL/6N mouse strains. Genome Biol 14:R82.
43. Brownley KA, Peat CM, La Via M, Bulik CM (2015): Pharmacological approaches to the management of binge eating disorder. Drugs 75: 9–32.
44. Smith KL, Rao RR, Velazquez-Sanchez C, Valenza M, Giuliano C, Everitt BJ, *et al*. (2015): The uncompetitive N-methyl-D-aspartate antagonist memantine reduces binge-like eating, food-seeking behavior, and compulsive eating: role of the nucleus accumbens shell. Neuropsychopharmacology 40:1163–1171.
45. Takenawa T, Suetsugu S (2007): The WASP-WAVE protein network: Connecting the membrane to the cytoskeleton. Nat Rev Mol Cell Biol 8:37–48.
46. Napoli I, Mercaldo V, Boyl PP, Eleuteri B, Zalfa F, De Rubeis S, *et al*. (2008): The fragile X syndrome protein represses activity-dependent translation through CYFIP1, a new 4E-BP. Cell 134:1042–1054.
47. Abekhoukh S, Bardoni B (2014): CYFIP family proteins between autism and intellectual disability: Links with Fragile X syndrome. Front Cell Neurosci 8:81.
48. Schenck A, Bardoni B, Moro A, Bagni C, Mandel JL (2001): A highly conserved protein family interacting with the fragile X mental retardation protein (FMRP) and displaying selective interactions with FMRP-related proteins FXR1P and FXR2P. Proc Natl Acad Sci U S A 98: 8844–8849.
49. Klump KL, Racine S, Hildebrandt B, Sisk CL (2013): Sex differences in binge eating patterns in male and female adult rats. Int J Eat Disord 46:729–736.
50. Babbs RK, Wojnicki FH, Corwin RL (2011): Effect of 2-hydroxyestradiol on binge intake in rats. Physiol Behav 103:508–512.
51. Reichelt AC, Abbott KN, Westbrook RF, Morris MJ (2016): Differential motivational profiles following adolescent sucrose access in male and female rats. Physiol Behav 157:13–19.
52. Asarian L, Geary N (2013): Sex differences in the physiology of eating. Am J Physiol Regul Integr Comp Physiol 305:R1215–R1267.
53. Ames SL, Kisbu-Sakarya Y, Reynolds KD, Boyle S, Cappelli C, Cox MG, *et al*. (2014): Inhibitory control effects in adolescent binge eating and consumption of sugar-sweetened beverages and snacks. Appetite 81:180–192.
54. Sinclair EB, Culbert KM, Gradl DR, Richardson KA, Klump KL, Sisk CL (2015): Differential mesocorticolimbic responses to palatable food in binge eating prone and binge eating resistant female rats. Physiol Behav 152:249–256.
55. Babbs RK, Unger EL, Corwin RL (2013): 2-Hydroxyestradiol enhances binge onset in female rats and reduces prefrontal cortical dopamine in male rats. Horm Behav 63:88–96.
56. Carroll ME, Smethells JR (2016): Sex differences in behavioral dyscontrol: Role in drug addiction and novel treatments. Front Psychiatry 6:175.
57. Parylak SL, Koob GF, Zorrilla EP (2011): The dark side of food addiction. Physiol Behav 104:149–156.
58. He X, Stefan M, Terranova K, Steinglass J, Marsh R (2016): Altered white matter microstructure in adolescents and adults with bulimia nervosa. Neuropsychopharmacology 41:1841–1848.
59. Mettler LN, Shott ME, Pryor T, Yang TT, Frank GK (2013): White matter integrity is reduced in bulimia nervosa. Int J Eat Disord 46: 264–273.
60. Frank GK (2015): Advances from neuroimaging studies in eating disorders. CNS Spectr 20:391–400.
61. Martin Monzon B, Hay P, Foroughi N, Touyz S (2016): White matter alterations in anorexia nervosa: A systematic review of diffusion tensor imaging studies. World J Psychiatry 6:177–186.
62. Berner LA, Avena NM, Hoebel BG (2008): Bingeing, self-restriction, and increased body weight in rats with limited access to a sweet-fat diet. Obesity (Silver Spring) 16:1998–2002.
63. Corwin RL (2006): Bingeing rats: A model of intermittent excessive behavior? Appetite 46:11–15.
64. Cottone P, Sabino V, Steardo L, Zorrilla EP (2008): Intermittent access to preferred food reduces the reinforcing efficacy of chow in rats. Am J Physiol Regul Integr Comp Physiol 295:R1066–R1076.
65. Fontaine DA, Davis DB (2016): Attention to background strain is essential for metabolic research: C57BL/6 and the International Knockout Mouse Consortium. Diabetes 65:25–33.
66. Heiker JT, Kunath A, Kosacka J, Flehmig G, Knigge A, Kern M, *et al*. (2014): Identification of genetic loci associated with different responses to high-fat diet-induced obesity in C57BL/6N and C57BL/6J substrains. Physiol Genomics 46:377–384.
67. Rendina-Ruedy E, Hembree KD, Sasaki A, Davis MR, Lightfoot SA, Clarke SL, *et al*. (2015): A comparative study of the metabolic and skeletal response of C57BL/6J and C57BL/6N mice in a diet-induced model of type 2 diabetes. J Nutr Metab 2015:758080.
68. Angulo MA, Butler MG, Cataletto ME (2015): Prader-Willi syndrome: A review of clinical, genetic, and endocrine findings. J Endocrinol Invest 38:1249–1263.
69. Dichter GS, Damiano CA, Allen JA (2012): Reward circuitry dysfunction in psychiatric and neurodevelopmental disorders and genetic syndromes: Animal models and clinical findings. J Neurodev Disord 4:19.
70. Butler MG, Bittel DC, Kibiryeva N, Talebizadeh Z, Thompson T (2004): Behavioral differences among subjects with Prader-Willi syndrome and type I or type II deletion and maternal disomy. Pediatrics 113:565–573.
71. Milner KM, Craig EE, Thompson RJ, Veltman MW, Thomas NS, Roberts S, *et al*. (2005): Prader-Willi syndrome: Intellectual abilities and behavioural features by genetic subtype. J Child Psychol Psychiatry 46:1089–1096.
72. Yalcin B, Wong K, Agam A, Goodson M, Keane TM, Gan X, *et al*. (2011): Sequence-based characterization of structural variation in the mouse genome. Nature 477:326–329.
73. Dougherty JD, Schmidt EF, Nakajima M, Heintz N (2010): Analytical approaches to RNA profiling data for the identification of genes enriched in specific cells. Nucleic Acids Res 38:4218–4230.